The Myoepithelial Cells of Salivary Intercalated Duct-type Intraductal Carcinoma Are Neoplastic

A Study Using Combined Whole-slide Imaging, Immunofluorescence, and RET Fluorescence In Situ Hybridization

Justin A. Bishop, MD, Lisa M. Rooper, MD,†‡ Ankur R. Sangoi, MD,§ Jeffrey Gagan, MD, PhD,* Lester D.R. Thompson, MD,|| and Hiroshi Inagaki, MD, PhD¶*

Abstract: Intraductal carcinoma (IDC) is a salivary gland tumor currently believed to be analogous to breast ductal carcinoma in situ, consisting of a complex neoplastic epithelial proliferation surrounded by a continuous layer of myoepithelial cells presumed to be native and non-neoplastic. Recent molecular insights have shown that there are at least 3 different types of IDC: (1) intercalated duct-like, with frequent *NCOA4-RET* fusions; (2) apocrine, with multiple mutations similar to salivary duct carcinoma; and (3) mixed intercalated duct-like and apocrine with frequent *RET* fusions, especially *TRIM27-RET*. Recent observations (eg, IDC occurring in lymph nodes) have challenged the notion that the myoepithelial cells of IDC are non-neoplastic. Five IDCs with known *RET* fusions by RNA sequencing were retrieved from the authors' archives, including 4 intercalated duct-like IDCs with *NCOA4-RET*, and 1 mixed intercalated duct-like/apocrine IDC with *TRIM27-RET*. A panel of immunohistochemistry antibodies (S100 protein, p63 or p40, mammaglobin, smooth muscle actin, calponin, androgen receptor) was tested. To precisely localize *RET* split-positive cells, each case was subjected to sequential retrieval of whole-slide imaging data of hematoxylin and eosin (HE) staining, immunofluorescence staining for calponin, and fluorescence in situ hybridization (FISH) for *RET*. Because *NCOA4-RET* is an inversion difficult to visualize on conventional *RET* FISH, a novel 3-color FISH technique was utilized to demonstrate it clearly. In all 5 cases, the proliferative ducts were completely surrounded by a layer of myoepithelial cells that were positive for p63 or p40, smooth muscle actin, and calponin. Using combined HE, calponin immunofluorescence, and *RET* FISH imaging, the positive signals were unmistakably identified in both calponin-negative ductal cells and peripheral, calponin-positive myoepithelial cells in all 5 cases. Utilizing combined HE, calponin immunofluorescence, and *RET* FISH imaging, we demonstrated that IDCs with *RET* fusions harbored this alteration in both the ductal and myoepithelial cells. This is compelling evidence that the myoepithelial cells of IDC are not mere bystanders, but are rather a component of the neoplasm itself, similar to other biphasic salivary gland neoplasms like pleomorphic adenoma and epithelial-myoepithelial carcinoma. This finding raises questions about the appropriate terminology, classification, and staging of IDC.

Key Words: salivary gland neoplasms, intraductal carcinoma, intercalated duct carcinoma, *NCOA4-RET*, *TRIM27-RET*

(*Am J Surg Pathol* 2021;45:507–515)

From the *Department of Pathology, UT Southwestern Medical Center, Dallas, TX; Departments of †Pathology; ‡Oncology, The Johns Hopkins Hospital, Baltimore, MD; §Department of Pathology, El Camino Hospital, Mountain View; ||Southern California Permanente Medical Group, Woodland Hills Medical Center, Woodland Hills, CA; and ¶Department of Pathology and Molecular Diagnostics, Graduate School of Medical Sciences, Nagoya City University, Nagoya, Japan.

Conflicts of Interest and Source of Funding: This study was supported in part by the Jane B. and Edwin P. Jenevein, MD Endowment for Pathology at UT Southwestern Medical Center. Supported in part by grants-in-aid for scientific research, MEXT, Japan to H.I. (No. 16H04713). The remaining authors have disclosed that they have no significant relationships with, or financial interest in, any commercial companies pertaining to this article.

Correspondence: Justin A. Bishop, MD, University of Texas Southwestern Medical Center, Clements University Hospital, UH04.250, 6201 Harry Hines Boulevard, Dallas, TX, 75390 (e-mail: justin.bishop@utsouthwestern.edu).

Supplemental Digital Content is available for this article. Direct URL citations appear in the printed text and are provided in the HTML and PDF versions of this article on the journal's website, www.ajsp.com.

BACKGROUND

Intraductal carcinoma (IDC) is a rare salivary gland neoplasm that has previously been known as "low-grade salivary duct carcinoma" and "low-grade cribriform cystadenocarcinoma".[1–5] The IDC terminology adopted in the most recent WHO Classification of Head and Neck Tumors was based on the notion that it is analogous to ductal carcinoma in situ of the breast: a mass-forming, neoplastic ductal epithelial proliferation growing within the preexisting salivary ductal system and surrounded by a continuous layer of myoepithelial cells presumed to be native and non-neoplastic.

Recent molecular advances have demonstrated that IDC is not a homogeneous entity but rather consists of at least 3 distinctive variants: (1) intercalated duct-like IDC,

which is positive for S100 protein and SOX10 and often harbors *NCOA4-RET*; (2) apocrine IDC, which is positive for androgen receptor (AR) and has a complex genetic profile including *HRAS* and *PIK3CA* hotspot mutations; and (3) hybrid or mixed IDC which demonstrates both intercalated duct-like and apocrine features and often has *RET* fusions, especially *TRIM27-RET*.[6–13] The apocrine variant is often high grade and frankly invasive, while the other 2 forms are usually low grade and only rarely show overt invasion.[10–12,14] When IDC is completely intraductal (ie, surrounded by myoepithelial cells), it has an excellent prognosis, while overtly invasive examples without myoepithelial cells often behave aggressively.[10–12,14]

Recent observations have raised doubts about the non-neoplastic nature of the myoepithelial cells in IDC, suggesting it is not truly analogous to breast ductal carcinoma in situ. First, there have been several reported cases of IDC involving intraparotid lymph nodes.[4,15–17] Second, there is a reported case of an oral cavity IDC invading into bone.[18]

We sought to determine whether the myoepithelial cells of IDC are neoplastic by localizing which cells (ductal, myoepithelial, or both) of fusion-positive IDCs harbor their defining fusions. While routine fluorescence in situ hybridization (FISH) does not allow for this kind of resolution, we employed a method previously described by Fujii et al,[19] where whole-slide imaging (WSI) data of hematoxylin and eosin (HE), immunofluorescence for calponin, and *RET* FISH was superimposed. We discuss the implications of these findings for diagnosis and classification.

METHODS

IDC Cases

After institutional review board approval, we identified cases of intercalated duct-type or mixed intercalated duct-like/apocrine IDC from the authors' consultation files. Three previously published cases had been shown to harbor *RET* fusions by next-generation sequencing and FISH.[10,12,17] Two new cases were subjected to targeted RNA sequencing as described previously.[20] Briefly, whole-slide tissue sections were cut at 10 μm, and Qiagen AllPrep kits (Qiagen, Germantown, MD) were used for RNA isolation. A sequencing library was generated using a modified TruSight RNA Pan-Cancer kit (Illumina, San Diego, CA) with 1425 genes. Sequencing was performed on the NextSeq. 550 (Illumina) with a minimum of 6 million mapped reads. Fusions are identified using the STAR-Fusion algorithm.[21] All fusions were manually reviewed via the Integrative Genomics Viewer (Broad Institute, Cambridge, MA).[22]

Immunohistochemistry

We performed immunohistochemistry for S100 protein (Ventana Medical Systems, Tucson, AZ), smooth muscle actin (Ventana Medical Systems), AR (Ventana Medical Systems) mammaglobin (Agilent-Dako, Carpinteria, CA), calponin (Agilent-Dako); and either p40 (BioCare Medical, Concord, CA) or p63 (BioCare) on all cases. Staining was performed on 4 μm whole-slide sections using standardized automated protocols on Ventana BenchMark Ultra autostainers (Ventana Medical Systems) in the presence of appropriate controls. These studies were performed on one representative block per case.

Sequential Retrieval of WSI Data of HE-stained and Immunofluorescence-stained Material, and FISH on Paraffin Sections

After deparaffinization, 1 tumor section of each case was stained with HE. WSI data of the HE section were obtained using an automated image analyzer (IN Cell Analyzer 6000; GE Healthcare, Little Chalfont, UK), which was equipped with a ×60 objective lens. The HE section was then subjected to immunofluorescence staining for calponin. The section was heat-treated to inactivate the HE dyes and for antigen retrieval in 10 mM citric acid buffer (pH 6.0). Next, it was reacted with anticalponin antibody (clone, CALP; Invitrogen, Waltham, MA), subsequently incubated with Alexa Fluor 555-labeled second antibody (Thermo Fisher Scientific, Tokyo, Japan), and was finally stained with diaminophenilindole. Immunofluorescence WSI data were obtained using the automated image analyzer. The immunofluorescence section was then subjected to tissue FISH analysis. Briefly, the section was heat-treated, digested in pepsin buffer, and incubated with 2 or 3 FISH probes overnight at 37°C in a humidified chamber. After posthybridization washes, the section was stained with diaminophenilindole. Alexa Fluor 555 signals for calponin were completely inactivated during the pretreatment process for FISH. FISH-WSI data were again obtained using the automated image analyzer. These staining and image-retrieval processes are shown in Figure 1.

Preparation of FISH Probes

The FISH probes that we used were prepared by labeling BAC clones (Supplemental Table 1, Supplemental Digital Content 1, http://links.lww.com/PAS/B27) for fluorescence dyes using a Nick Translation Reagent kit (Abbott, Abbott Park, IL). For the case with *TRIM27-RET* resulting from t(6;10)(p22;q11), we used a break-apart FISH assay, where probes encompassing *RET* that were labeled for either FITC or rhodamine. For the cases

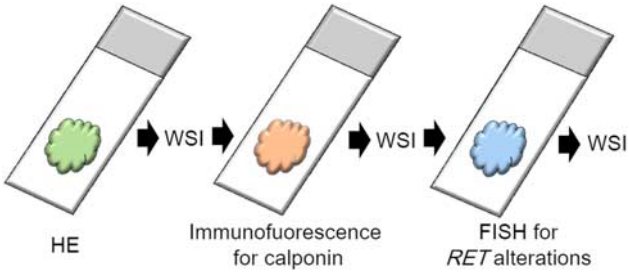

FIGURE 1. Sequential retrieval of WSI data of HE staining, immunofluorescence staining for calponin, and FISH for *RET* alterations.

with *NCOA4-RET*, a novel 3-color technique was used since *RET* and *NCOA4* genes are located close to each other (separated by ~3 Mbp). For this technique (inversion FISH), we prepared another FISH probe in addition to the above mentioned 2 FISH probes. This probe targeted the center area between *RET* and *NCOA4*, and labeled for Cy5 (Supplemental Table 1, Supplemental Digital Content 1, http://links.lww.com/PAS/B27, Fig. 2). The FITC, rhodamine, and Cy5 signals were visualized in green, red, and blue, respectively.

WSI Data Processing

Small image tiles obtained with the automated image analyzer were stitched together into a large contiguous montage using image analysis software, Image J (version 1.52), on a high-performance computer. To detect *RET* alterations at the cellular level, we first identified tumor ductal and myoepithelial cells using HE and calponin-immunofluorescence images. The presence or absence of *RET* alterations in the ductal and myoepithelial cells was determined by carefully analyzing the FISH images superimposed on the HE and calponin-immunofluorescence images.

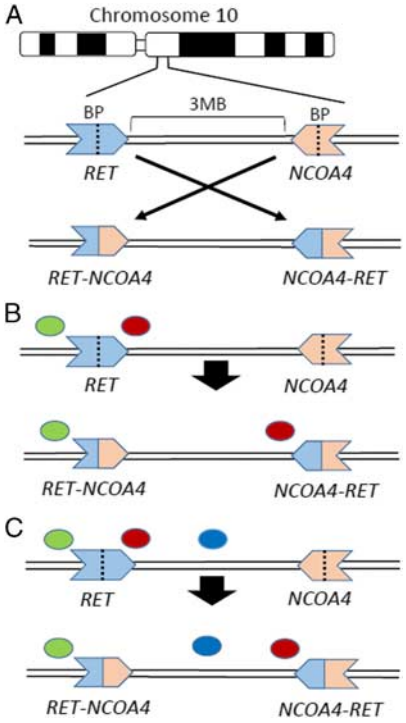

FIGURE 2. The *NCOA4-RET* fusion present in 4 of the IDCs is an inversion of genes that are only 3 Mbp apart (A). This alteration is very difficult to visualize with traditional 2-color *RET* break-apart FISH, where the separation of red and green signals is very subtle (B). For these cases, a novel 3-color technique was used (inversion FISH), where a FISH probe with a blue signal targeting the center area between *RET* and *NCOA4* was added. In this assay (C), normal cells have a green-red-blue arrangement, while cells with the *NCOA4-RET* fusion have a green-blue-red arrangement.

RESULTS

Five IDCs with *RET* fusions were identified. The clinical and demographic information for these cases are summarized in Table 1. The IDCs included 4 intercalated duct-type IDCs with *NCOA4-RET*, and 1 mixed intercalated duct-like/apocrine IDC with *TRIM27-RET* (Fig. 3). The tumors arose in 4 men and 1 woman, ranging from 50 to 79 years (mean, 65 y). Each patient presented with a mass or slow-growing swelling in the parotid gland region which had been resected. Four of the cases were centered in the parotid gland, while 1 case arose in an intraparotid lymph node. The tumors had an average size of 1.6 cm (range, 0.9 to 2.8 cm). Three patients with follow-up information had not developed recurrence or metastasis after an average of 32 months (range, 22 to 44 mo).

Histologically, all 5 lesions consisted of complex epithelial proliferations made up of tubules, solid nests, cribriform, and micropapillary structures with extensive cyst formation (Fig. 4A). The tumor nests were smooth and rounded, and in many areas a rim of compressed myoepithelial cells could be seen. There were no irregular nests or desmoplasia to suggest overt stromal invasion. All tumors had intercalated duct-like tumor cells with abundant eosinophilic to amphophilic cytoplasm and bland oval nuclei with delicate chromatin and indistinct nucleoli (Fig. 4B). The mixed intercalated duct-like/apocrine IDC had 2 components: intercalated duct-like cells, and apocrine cells with abundant granular eosinophilic cytoplasm and large nuclei with prominent nucleoli (Fig. 4C). All of the IDCs were histologically low grade.

The immunohistochemical findings are summarized in Table 2. The intercalated duct-like IDCs were diffusely positive for S100 protein (Fig. 4D) and mammaglobin, and negative for AR. The one mixed intercalated duct-like/apocrine IDC was positive for S100 protein and mammaglobin and negative for AR in the intercalated duct-like component, with the inverse staining pattern in the apocrine component (Fig. 4E). In all 5 cases, the proliferative ducts were completely surrounded by a layer of myoepithelial cells that were positive for p63 or p40 (Fig. 4F), smooth muscle actin, and calponin.

Using a single formalin-fixed paraffin-embedded section of each tumor case, the WSI data of HE staining, immunofluorescence staining for calponin, and FISH for *RET* rearrangement were sequentially retrieved (Fig. 5). Using this method, signal patterns indicating *RET* rearrangement were unmistakably present in both calponin-negative ductal cells and peripheral, calponin-positive myoepithelial cells in all 5 cases (Supplemental Table 2, Supplemental Digital Content 2, http://links.lww.com/PAS/B28). The alteration was identified in 10.3% to 33.4% of myoepithelial cells (mean, 19.6%). For the case with *TRIM27-RET*, a classic split was identified on break-apart FISH (Figs. 3, 6). For the remaining cases with *NCOA4-RET*, a 3-color inversion FISH technique was required to demonstrate the fusion because *NCOA4-RET* is an inversion that is very difficult to visualize on routine *RET* break-apart FISH (Figs. 3, 7). Surrounding stromal

TABLE 1. Clinical and Demographic Information

Case No.	Age (y)	Sex	Presentation	Size (cm)	Diagnosis	Follow-up
1	66	Male	Right parotid mass	1.3	Mixed intercalated duct/apocrine-type IDC involving parotid	NED at 30 mo
2	62	Female	Left parotid mass	0.9	Intercalated duct-type IDC involving parotid	NA
3	68	Male	Right parotid mass	2.8	Intercalated duct-type IDC involving intraparotid LN	DOC at 44 mo, NED
4	79	Male	Right parotid mass	1.8	Intercalated duct-type IDC involving parotid with TALP	NED at 22 mo
5	50	Male	Left parotid mass	1.0	Intercalated duct-type IDC involving parotid with TALP	NA

DOC indicates dead of other causes; LN, lymph node; NA, not available; NED, no evidence of disease; TALP, tumor-associated lymphoid proliferation.

cells and lymphocytes were negative for *RET* fusions, providing an internal control.

DISCUSSION

Molecular testing has recently shed considerable light on the rare salivary gland tumor known as IDC. We now know that IDC consists of at least 3 subtypes, each with unique histologic, immunophenotypic, and molecular features. Intercalated duct-type IDC is most common. It is diffusely positive for S100 protein and SOX10, negative for AR, and commonly harbors *NCOA4-RET* (in up to half of reported cases).[10–12] Rare cases have had alternate fusions like *STRN-ALK*, *TUT1-ETV5*, and *KIAA1217-RET*, and in some cases a fusion has not been identified.[10,17] The apocrine variant of IDC is strongly positive for AR and negative for S100 protein and SOX10. It has not been found to harbor fusions, but instead, has been shown to have a complex mutational profile (eg, *PIK3CA* and *HRAS* mutations, *TP53* loss), similar to salivary duct carcinoma.[6,8,11,12] Finally, the mixed intercalated duct/apocrine variant of IDC has mixed or hybrid

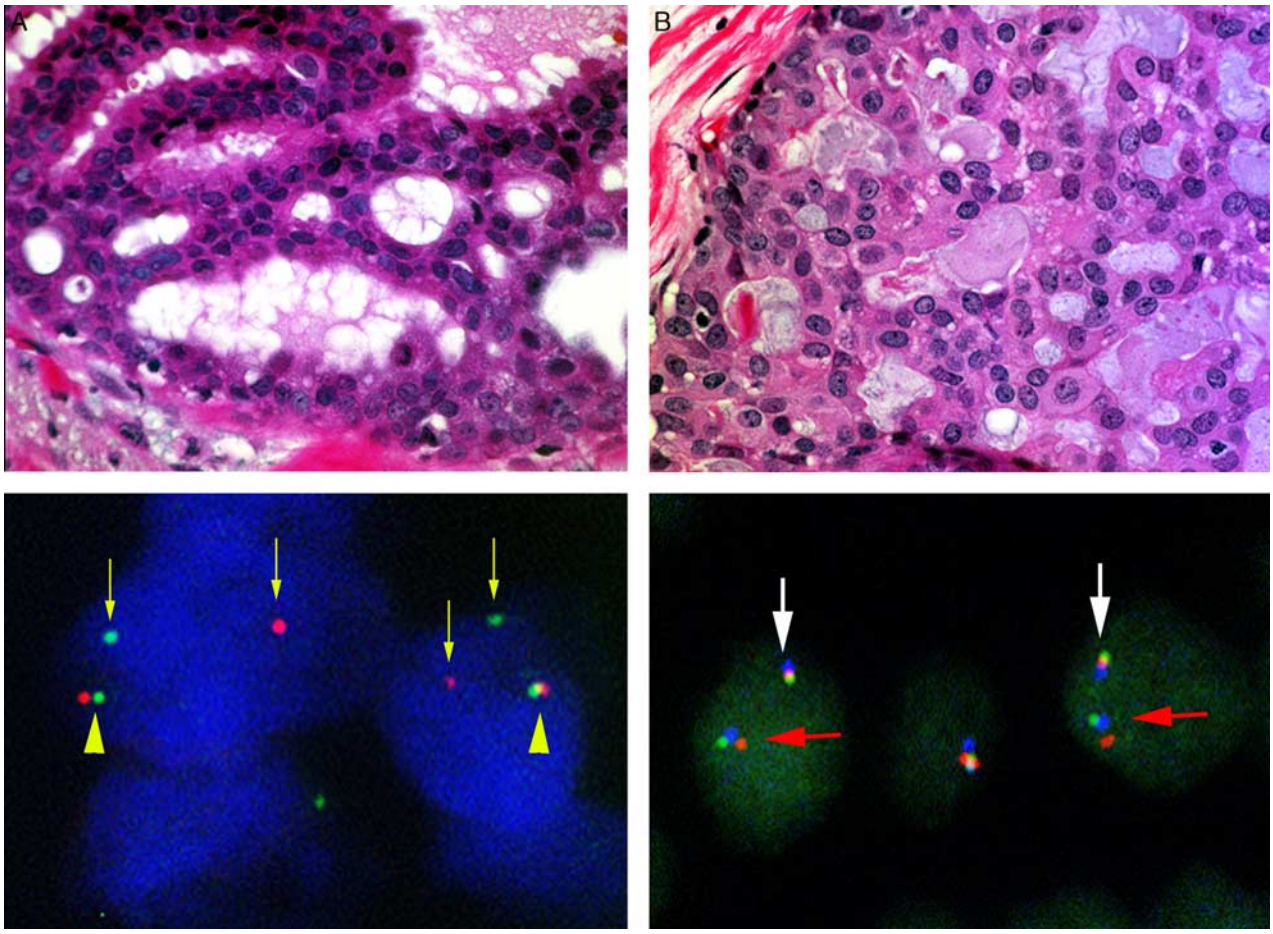

FIGURE 3. One IDC (A) had a *TRIM27-RET* fusion which was visualized as a traditional split on break-apart *RET* FISH. Cells had 1 intact copy (arrowheads) and 1 split apart (arrows) (B). The remaining 4 IDCs had an *NCOA4-RET* fusion, which was visualized on 3-color inversion FISH. Cells had 1 normal copy (green-red-blue signals, white arrows) and 1 rearranged (green-blue-red signals, red arrows).

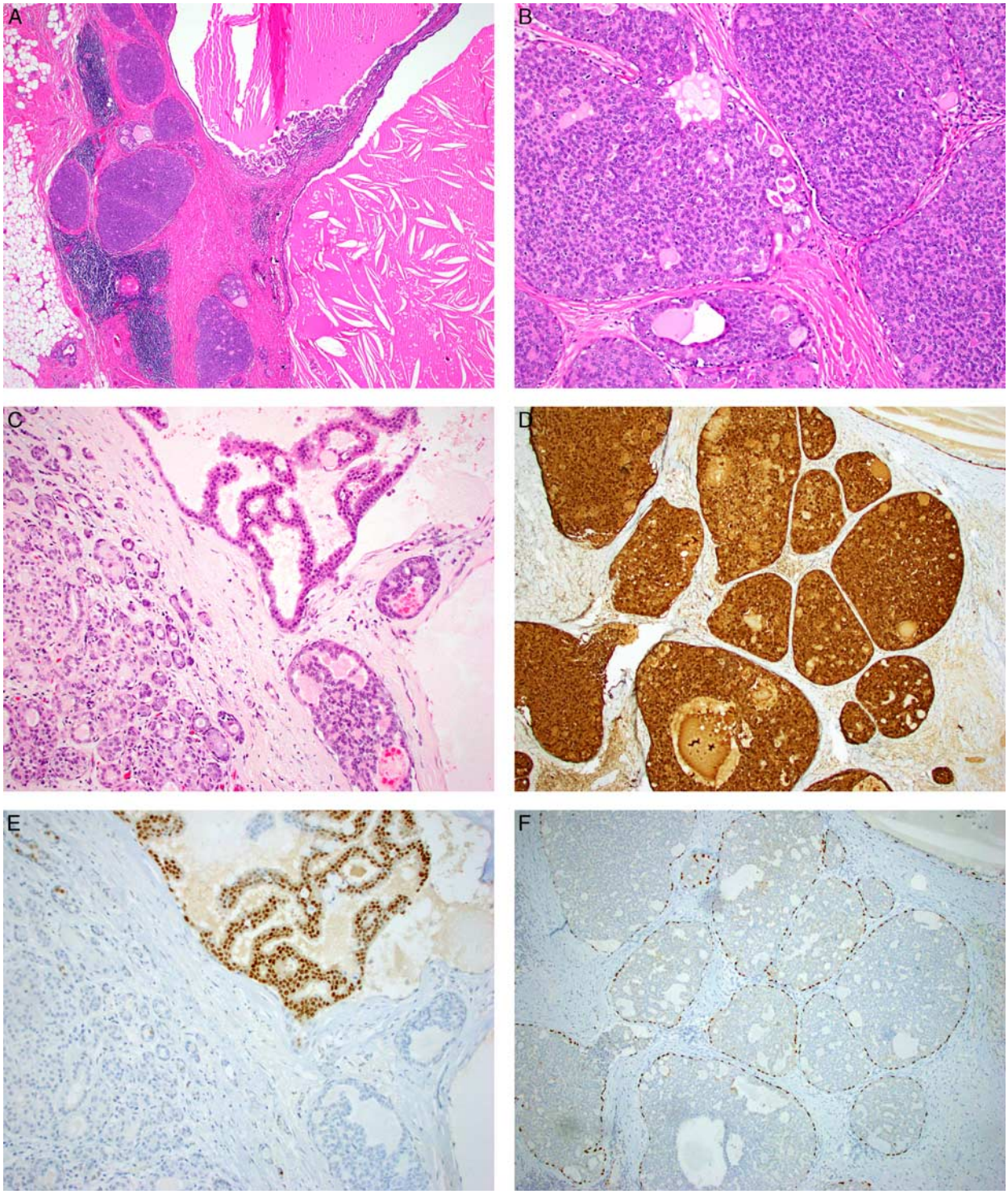

FIGURE 4. The IDCs were well-circumscribed and consisted of large cysts adjacent to solid nodules (A). The tumors were composed of solid or cribriform nests with rounded, smooth borders. The intercalated duct-type cells were uniform oval cells with moderate eosinophilic cytoplasm. Very small, clear cell myoepithelial cells were subtly visible at the edge of the nests (B). The 1 mixed IDC had distinct areas of apocrine differentiation (top) among the intercalated duct-like areas. (C). All cases had intercalated duct-type differentiation with diffuse expression of S100 protein (D). The 1 mixed case showed strong AR staining in the apocrine tumor component (E). In all cases, the nests were entirely surrounded by small myoepithelial cells that were positive for either p40 (shown here) or p63 (F).

TABLE 2. Immunohistochemical Results

Case No.	S100 Protein	Mammaglobin	p63/p40	SMA	Calponin	AR
1	Positive in intercalated duct-like areas, negative in apocrine areas	Positive in intercalated duct-like areas, negative in apocrine areas	Peripheral	Peripheral	Peripheral	Positive in apocrine areas, negative in intercalated duct-like areas
2	Diffusely positive	Diffusely positive	Peripheral	Peripheral	Peripheral	Negative
3	Diffusely positive	NA	Peripheral	Peripheral	Peripheral	Negative
4	Diffusely positive	Diffusely positive	Peripheral	Peripheral	Peripheral	Negative
5	Diffusely positive	Diffusely positive	Peripheral	Peripheral	Peripheral	Negative

NA indicates not available; SMA, smooth muscle actin.

histologic and immunophenotypic features of both other IDC types. Like pure intercalated duct-like IDC, mixed IDC also commonly harbors *RET* fusions, although *TRIM27-RET* is the most common fusion in this variant.[9–11] An oncocytic variant of IDC has also been rarely reported, although it is not yet established if this is a distinct variant or merely metaplastic changes in intercalated duct-like IDC.[23]

All forms of IDC are characterized by complex ductal proliferations surrounded by an intact layer of myoepithelial cells. Cases of intercalated duct-like and apocrine IDC with frank stromal invasion accompanied by a loss of myoepithelial cells have been reported.[10,12] This phenomenon is common in apocrine IDC, but uncommon in the intercalated duct and mixed types. When IDC (of all types) is completely surrounded by myoepithelial cells, it has an excellent prognosis, with only rare recurrences and no risk of metastasis. In contrast, when frank invasion is present, these tumors can be clinically aggressive. These clinical findings, combined with histologic similarities, have resulted in the assumption that IDC is the salivary gland equivalent to ductal carcinoma in situ of the breast. Indeed, the current classification of salivary gland tumors regards IDC as a neoplastic proliferation growing within the preexisting system of salivary ducts.[5] It is accordingly staged as in situ disease (pTis) in current salivary gland staging protocols.[24]

Some recent observations have cast doubt, however, on the belief that salivary IDC is analogous to breast ductal carcinoma in situ. First, there have been several reported cases of IDC involving intraparotid lymph nodes.[4,15–17] While many salivary gland tumors have been reported to arise from benign parotid gland inclusions in intraparotid gland lymph nodes, it strains believability that the sheer number of myoepithelial cells seen in intranodal IDCs can exist normally within microscopic intranodal inclusions. Second, an oral cavity IDC has been reported with extension into bone.[18] This finding is very difficult to explain as growth within preexisting ducts, as there are no normal ducts or myoepithelial cells within bone.

Using combined HE staining, calponin immunofluorescence, and *RET* FISH imaging on 5 cases of IDC known to harbor *RET* fusions, we found that these characteristic fusions were present not only in the luminal ductal cells as expected, but also the surrounding myoepithelial cells. This is compelling evidence that for IDC, both the ductal cells and the surrounding myoepithelial cells are clonal and neoplastic. This finding strongly refutes the prevailing notion that IDC grows within preexisting, native ducts, and helps explain the reports of IDC within lymph nodes and bone. At the same time, the concept of neoplastic myoepithelial cells in IDC raises additional questions about classification, nomenclature and staging.

Many salivary gland carcinomas such as epithelial-myoepithelial carcinoma, adenoid cystic carcinoma, and basal cell adenocarcinoma are biphasic and composed of both ductal and myoepithelial cells, with both populations neoplastic and frankly invasive. In contrast, benign salivary gland tumors such as pleomorphic adenoma also have neoplastic ducts and myoepithelial cells. It is unclear where on this spectrum IDC falls. It is possible that IDC is a very low grade and indolent biphasic invasive carcinoma with a pushing border. This would explain the rare occurrence of IDC within bone. If this is the case, the phenomenon of frank invasion with myoepithelial cell loss could be similar to high-grade transformation seen in other salivary gland tumors. Indeed, in adenoid cystic carcinomas with high-grade transformation, the myoepithelial cell component is lost.[25] It is also possible that the intraluminal ductal component of IDC truly is an "in situ" carcinoma within a preexisting benign precursor neoplasm, similar to noninvasive salivary duct carcinoma arising in a preexisting pleomorphic adenoma or within sclerosing polycystic adenoma.[20] In a case of noninvasive salivary duct carcinoma arising in a *PLAG1*-rearranged pleomorphic adenoma, for example, both the ductal and myoepithelial cells would be positive for *PLAG1* rearrangements by FISH but the neoplastic ductal cells in this scenario would be malignant, while the neoplastic myoepithelial cells would be benign. Unlike other biphasic salivary gland carcinomas, the myoepithelial cells seen in IDC are very small and inconspicuous, with no cellular atypia or appreciable mitotic activity. While an IDC with myoepithelial cells in bone is difficult to explain if it is simply carcinoma in situ, occasionally benign neoplasms can erode into bone (eg, inverted sinonasal papillomas, meningiomas, nasopharyngeal angiofibromas). In this carcinoma in situ scenario, cases showing loss of myoepithelial cells would truly represent invasion from a precursor neoplasm, similar to invasive carcinomas ex-pleomorphic adenoma. Separating between these 2 possibilities will be difficult or impossible, and it remains a

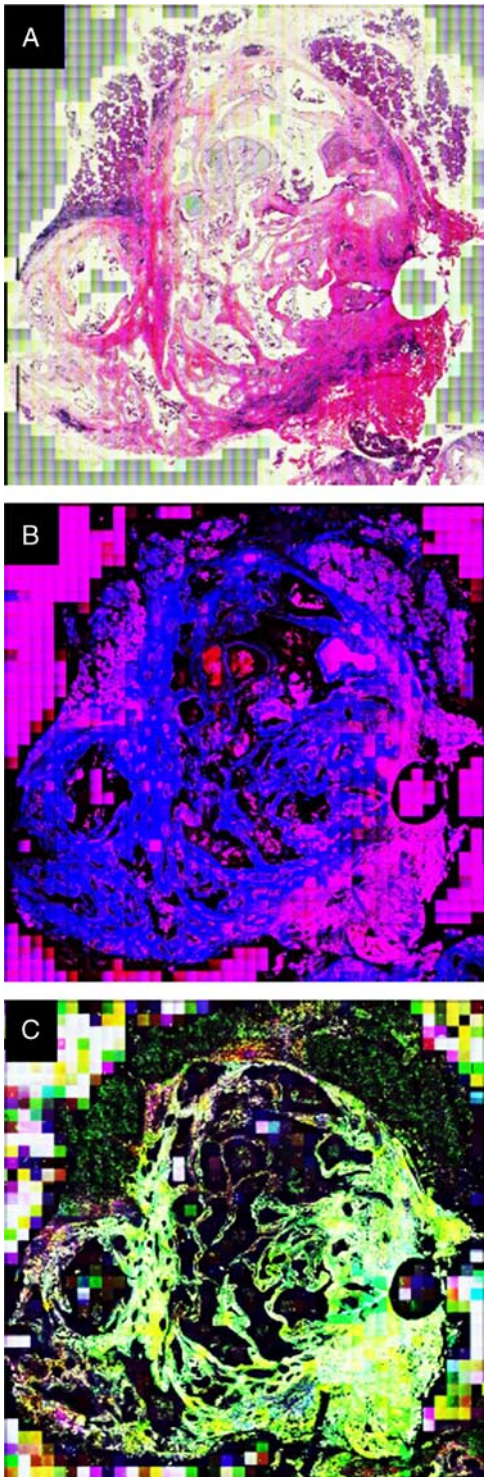

FIGURE 5. Sequential retrieval of WSI data of HE staining (A), immunofluorescence staining for calponin (B), and FISH for *RET* (C).

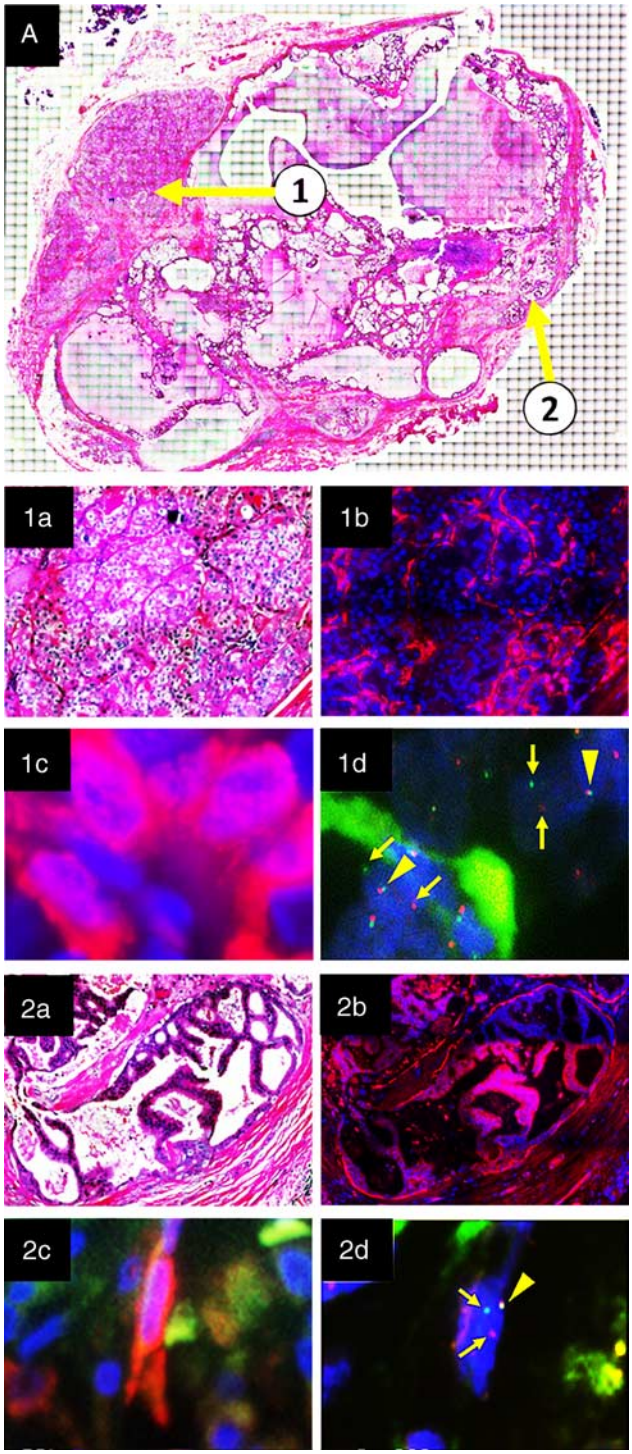

FIGURE 6. This IDC had a *TRIM27-RET* fusion. HE-stained section demonstrates 2 areas (1, 2) (A). Matched HE (1a, 2a) and calponin immunofluorescence (red fluorophore) at low power (1b, 2b), and matched calponin immunofluorescence (red fluorophore) at high power (1c, 2c) and *RET* break-apart FISH (1d, 2d). Within the red calponin-positive myoepithelial cells, there is 1 intact *RET* gene (red and green signals together, arrowheads), and 1 rearranged *RET* gene (red and green signals split apart, arrows).

matter of debate whether the term "intraductal carcinoma" or staging as Tis is still appropriate. To this end, Skálová et al[10] proposed utilizing the term "intercalated

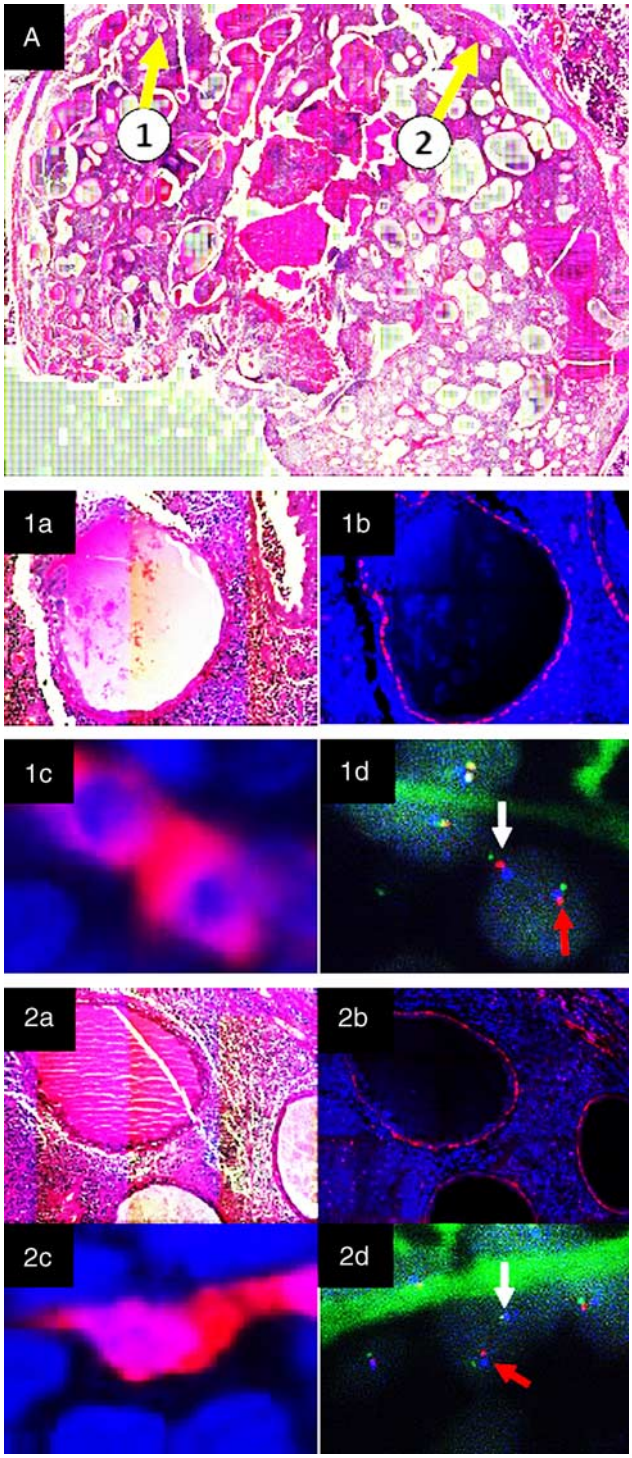

FIGURE 7. This IDC had a *NCOA4-RET* fusion. HE-stained section demonstrates 2 areas (1, 2) (A). Matched HE (1a, 2a) and calponin immunofluorescence (red fluorophore) at low power (1b, 2b), and matched calponin immunofluorescence (red fluorophore) at high power (1c, 2c) and inversion *RET* FISH (1d, 2d). Within the red calponin-positive myoepithelial cells, there is 1 intact *RET* gene (green-red-blue signals, white arrows), and 1 rearranged *RET* gene (green-blue-red signals, red arrows).

duct carcinoma" for IDC, subdividing cases into non-invasive (with myoepithelial cells) or invasive (no myoepithelial cells).

It is important to note that this study only examined intercalated duct-like and hybrid intercalated duct/apocrine IDCs. Purely apocrine IDCs lack characteristic gene fusions, and thus cannot be evaluated with the techniques employed in this study. Because they are histologically, immunophenotypically, and genetically different from the other forms of IDC, it is possible that the myoepithelial cells seen in apocrine IDC are indeed non-neoplastic, and that this form truly represents the analog of apocrine ductal carcinoma in situ of the breast. One possible strategy to answer this question could involve double staining with p40 and the *NRAS* Q61R antibody which cross-reacts with apocrine IDCs that harbor *HRAS* Q61R mutations.[8] In the future, apocrine IDC may be better regarded as a distinct entity.

The novel 3-color inversion FISH assay used in this study offers an exciting approach to testing for *RET* fusions in IDC. The most common *NCOA4-RET* fusion in IDC is a subtle intrachromosomal inversion that is easy to miss on conventional break-apart *RET* FISH. As a result, false negative results are common, and it is likely that the reported rate of *RET* fusions in intercalated duct-like IDC is lower than it truly is.[7,8,10–12] Utilizing the approach included here can give more reliable *RET* results for IDC without having to resort to expensive sequencing techniques. A similar FISH approach could also be used for other fusion-associated tumors harboring cryptic inversions.[26]

In summary, this study demonstrated that both the ductal and myoepithelial cells of a series of IDC harbored the same *RET* fusions, providing strong evidence that both cell types are neoplastic. As a result, intercalated duct and mixed IDCs should be regarded as biphasic salivary gland neoplasms. Questions remain about the malignant potential, terminology, and staging of IDC, which will require additional experience, study, and discussion.

ACKNOWLEDGMENTS

The authors thank Dr Jonathan Tobias for submitting a case and providing clinical information. They also thank Takeo Sakakibara for his excellent technical assistance.

REFERENCES

1. Brandwein-Gensler M, Gnepp DR. Low-grade cribriform cystadenocarcinoma. In: Barnes L, Eveson JW, Reichart P, Sidransky D, eds. *Pathology and Genetics of Head and Neck Tumours: World Health Organization Classification of Tumours*. Lyon, France: IARC; 2005:430.
2. Brandwein-Gensler M, Hille J, Wang BY, et al. Low-grade salivary duct carcinoma: description of 16 cases. *Am J Surg Pathol*. 2004;28:1040–1044.
3. Chen KT. Intraductal carcinoma of the minor salivary gland. *J Laryngol Otol*. 1983;97:189–191.
4. Delgado R, Klimstra D, Albores-Saavedra J. Low grade salivary duct carcinoma. A distinctive variant with a low grade histology and a predominant intraductal growth pattern. *Cancer*. 1996;78:958–967.
5. Loening T, Leivo I, Simpson RHW, et al. Intraductal carcinoma. In: El-Naggar A, Chan JK, Grandis JR, Takata T, Slootweg PJ, eds.

WHO Classification of Head and Neck Tumours. Lyon, France: International Agency for Research on Cancer; 2017:170–171.
6. Bishop JA, Gagan J, Krane JF, et al. Low-grade apocrine intraductal carcinoma: expanding the morphologic and molecular spectrum of an enigmatic salivary gland tumor. *Head Neck Pathol*. 2020. [Online ahead of print].
7. Guilmette J, Dias-Santagata D, Nose V, et al. Novel gene fusions in secretory carcinoma of the salivary glands: enlarging the ETV6 family. *Hum Pathol*. 2019;83:50–58.
8. Hsieh MS, Lee YH, Jin YT, et al. Clinicopathological study of intraductal carcinoma of the salivary gland, with emphasis on the apocrine type. *Virchows Arch*. 2020;477:581–592.
9. Lu H, Graham RP, Seethala R, et al. Intraductal carcinoma of salivary glands harboring TRIM27-RET fusion with mixed low grade and apocrine types. *Head Neck Pathol*. 2020;14:239–245.
10. Skálová A, Ptakova N, Santana T, et al. NCOA4-RET and TRIM27-ret are characteristic gene fusions in salivary intraductal carcinoma, including invasive and metastatic tumors: is "intraductal" correct? *Am J Surg Pathol*. 2019;43:1303–1313.
11. Skálová A, Vanecek T, Uro-Coste E, et al. Molecular profiling of salivary gland intraductal carcinoma revealed a subset of tumors harboring NCOA4-RET and novel TRIM27-RET fusions: a report of 17 cases. *Am J Surg Pathol*. 2018;42:1445–1455.
12. Weinreb I, Bishop JA, Chiosea SI, et al. Recurrent RET gene rearrangements in intraductal carcinomas of salivary gland. *Am J Surg Pathol*. 2018;42:442–452.
13. Weinreb I, Tabanda-Lichauco R, Van der Kwast T, et al. Low-grade intraductal carcinoma of salivary gland: report of 3 cases with marked apocrine differentiation. *Am J Surg Pathol*. 2006;30:1014–1021.
14. Simpson RH, Desai S, Di Palma S. Salivary duct carcinoma in situ of the parotid gland. *Histopathology*. 2008;53:416–425.
15. Lin SC, Ko RT, Kang BH, et al. Intraductal carcinoma of salivary gland originating from an intraparotid lymph node: a case report. *Malays J Pathol*. 2019;41:207–211.
16. Weinreb I. Intraductal carcinoma of salivary gland (so-called low-grade cribriform cystadenocarcinoma) arising in an intraparotid lymph node. *Head Neck Pathol*. 2011;5:321–325.
17. Rooper LM, Thompson LDR, Gagan J, et al. Salivary intraductal carcinoma arising within intraparotid lymph node: a report of 4 cases with identification of a novel STRN-ALK fusion. *Head Neck Pathol*. 2020. [Online ahead of print].
18. Todorovic E, Weinreb I. Intraductal carcinoma. *Surg Pathol Clin*. 2020. [In press].
19. Fujii K, Ishibashi KI, Kato J, et al. Cellular-level characterization of B cells infiltrating pulmonary MALT lymphoma tissues. *Virchows Arch*. 2016;469:575–580.
20. Bishop JA, Gagan J, Baumhoer D, et al. Sclerosing polycystic "adenosis" of salivary glands: a neoplasm characterized by PI3K pathway alterations more correctly named sclerosing polycystic adenoma. *Head Neck Pathol*. 2020;14:630–636.
21. Haas BJ, Dobin A, Li B, et al. Accuracy assessment of fusion transcript detection via read-mapping and de novo fusion transcript assembly-based methods. *Genome Biol*. 2019;20:213.
22. Robinson JT, Thorvaldsdottir H, Wenger AM, et al. Variant review with the Integrative Genomics Viewer. *Cancer Res*. 2017;77:e31–e34.
23. Nakaguro M, Urano M, Suzuki H, et al. Low-grade intraductal carcinoma of the salivary gland with prominent oncocytic change: a newly described variant. *Histopathology*. 2018;73:314–320.
24. Seethala R, Weinreb I, Bullock MJ, et al. Protocol for the examination of specimens from patients with carcinomas of the major salivary glands. 2018. Available at: https://documents.cap.org/protocols/cp-headandneck-larynx-17protocol-4001.pdf2017. Accessed September 1, 2020.
25. Seethala RR, Hunt JL, Baloch ZW, et al. Adenoid cystic carcinoma with high-grade transformation: a report of 11 cases and a review of the literature. *Am J Surg Pathol*. 2007;31:1683–1694.
26. Argani P, Zhang L, Reuter VE, et al. RBM10-TFE3 renal cell carcinoma: a potential diagnostic pitfall due to cryptic intrachromosomal Xp11.2 inversion resulting in false-negative TFE3 FISH. *Am J Surg Pathol*. 2017;41:655–662.